JOURNAL OF GEOPHYSICAL RESEARCH, VOL. 112, E08S17, doi:10.1029/2007JE002902, 2007

On the origin of perennial water ice at the south pole of Mars: A precession-controlled mechanism?

F. Montmessin,[1,2] R. M. Haberle,[1] F. Forget,[3] Y. Langevin,[4] R. T. Clancy,[5,6] and J.-P. Bibring[4]

Received 8 February 2007; revised 24 April 2007; accepted 2 August 2007; published 28 August 2007.

[1] The poles of Mars are known to have recorded recent ($<10^7$ years) climatic changes. While the south polar region appears to have preserved its million-year-old environment from major resurfacing events, except for the small portion containing the CO_2 residual cap, the discovery of residual water ice units in areas adjacent to the cap provides compelling evidence for recent glaciological activity. The mapping and characterization of these H_2O-rich terrains by Observatoire pour la Minéralogie, l'Eau, les Glaces et l'Activité (OMEGA) on board Mars Express, which have supplemented earlier findings by Mars Odyssey and Mars Global Surveyor, have raised a number of questions related to their origin. We propose that these water ice deposits are the relics of Mars' orbit precession cycle and that they were laid down when perihelion was synchronized with northern summer, i.e., more than 10,000 years ago. We favor precession over other possible explanations because (1) as shown by our General Circulation Model (GCM) and previous studies, current climate is not conducive to the accumulation of water at the south pole due to an unfavorable volatile transport and insolation configuration, (2) the residual CO_2 ice cap, which is known to cold trap water molecules on its surface and which probably controls the current extent of the water ice units, is geologically younger, (3) our GCM shows that 21,500 years ago, when perihelion occurred during northern spring, water ice at the north pole was no longer stable and accumulated instead near the south pole with rates as high as 1 mm yr^{-1}. This could have led to the formation of a meters-thick circumpolar water ice mantle. As perihelion slowly shifted back to the current value, southern summer insolation intensified and the water ice layer became unstable. The layer recessed poleward until the residual CO_2 ice cover eventually formed on top of it and protected water ice from further sublimation. In this polar accumulation process, water ice clouds play a critical role since they regulate the exchange of water between hemispheres. The so-called "Clancy effect," which sequesters water in the spring/summer hemisphere coinciding with aphelion due to cloud sedimentation, is demonstrated to be comparable in magnitude to the circulation bias forced by the north-to-south topographic dichotomy. However, we predict that the response of Mars' water cycle to the precession cycle should be asymmetric between hemispheres not only because of the topographic bias in circulation but also because of an asymmetry in the dust cycle. We predict that under a "reversed perihelion" climate, dust activity during northern summer is less pronounced than during southern summer in the opposite perihelion configuration (i.e., today's regime). When averaged over a precession cycle, this reduced potential for dust lifting will force a significantly colder summer in the north and, by virtue of the Clancy effect, will curtail the ability of the northern hemisphere to transfer volatiles to the south. This process may have helped create

[1]Space Science Division, NASA Ames Research Center, Moffett Field, USA.
[2]Now at Service d'Aéronomie, Centre National de la Recherche Scientifique, Institut Pierre-Simon Laplace, Université de Versailles Saint-Quentin-en-Yvelines, Verrières le Buisson, France.
[3]Laboratoire de Météorologie Dynamique, CNRS, IPSL, UPMC, Paris, France.
[4]Institut d'Astrophysique Spatiale, Orsay Campus, France.
[5]Space Science Institute, Boulder, Colorado, USA.
[6]Now at Space Science Institute, Bald Head Island, North Carolina, USA.

0148-0227/07/2007JE002902$09.00

the observed morphological differences in the layered deposits between the poles and could help explain the large disparity in their resurfacing ages.

Citation: Montmessin, F., R. M. Haberle, F. Forget, Y. Langevin, R. T. Clancy, and J.-P. Bibring (2007), On the origin of perennial water ice at the south pole of Mars: A precession-controlled mechanism?, *J. Geophys. Res.*, *112*, E08S17, doi:10.1029/2007JE002902.

1. Introduction

[2] The poles of Mars are covered with vast icy areas, the residual caps, whose composition, dimension and history differ significantly. The north pole has a dome of water ice [*Kieffer et al.*, 1976] which expands to a latitude of ~80°N and whose surface area is 5–10 times larger than that of the south. The residual cap in the north grades into the underlying layered materials whereas the south residual cap (SRC) remains markedly distinct from the surrounding layered terrains. The SRC is offset by 3° from the pole, confined inside the [0, 90W] longitudinal sector, possibly resulting from a bias in the deposition pattern forced by the Hellas basin [*Colaprete et al.*, 2005], and is not observed north of 85°S. Remote sensing of the SRC surface indicates temperatures buffered all year at the CO_2 phase change temperature (~140 K), providing evidence for a carbon dioxide composition [*Kieffer*, 1979]. In addition to CO_2 ice, recent observations made by the Mars Global Surveyor (MGS) and Mars Express (MEX) orbiters have revealed the existence of previously undetected portions of perennial water ice [*Titus et al.*, 2003; *Bibring et al.*, 2004]. With its imaging capability in the near-infrared, a spectral range where CO_2 and H_2O ice signatures can be unambiguously discriminated, the Observatoire pour la Minéralogie, l'Eau, les Glaces et l'Activité (OMEGA) instrument on MEX has mapped several of these water ice units: (1) Unit 1 is found within the bright CO_2 residual cap and shows water ice mixed with CO_2 ice. (2) Unit 2 forms a dark, CO_2-free, water ice strip, which outlines the scarps of the SRC and expands from underneath the thin and bright CO_2 cover of the cap. (3) Unit 3 consists of isolated water ice portions which are free of CO_2 and which are located at some distance from the SRC.

[3] These observations show that the SRC not only consists of permanent CO_2 ice but also encompasses areas of perennial H_2O ice without CO_2. The discovery of unit 1 has confirmed the long-standing hypothesis that the residual CO_2 acts as a permanent cold trap for water. With the surface temperature of the cap thermodynamically maintained at the CO_2 frost point, wet air masses flowing over the surface are cooled down to such temperatures that even marginal concentrations of water vapor exceed saturation and precipitate to the surface. This explains why H_2O ice is also observed within the CO_2 ice portion of the SRC. Cold trapping of water by CO_2 has, however, no direct role in the existence of the other units since only water ice is exposed there. Other modes of ice accumulation must be involved.

[4] As stated by *Bibring et al.* [2004], locations of units 2 and 3 refer to the same geological unit (Af) of the U.S. Geological Survey (USGS) I-2686 geological map (Figure 1) which was originally interpreted as partial CO_2 frost covered terrains. OMEGA data show that units 2 and 3 exhibit similar water ice/dust composition. Does it imply they also share the same history? The fact that polygonal sublimation features can be seen extending from inside the H_2O-rich unit 2 terrains to below the CO_2 ice layer in a transition zone located at the border of the residual CO_2 portion suggests that unit 2 is only the contour of a water ice layer residing under the CO_2 ice cap. Furthermore, the absence of slope change in the transition zone also suggests that the CO_2 veneer of the cap is probably not thicker than a few meters [*Bibring et al.*, 2004], supporting the modeling study of the "Swiss cheese holes" of the SRC by *Byrne and Ingersoll* [2003], who reached a similar conclusion. In such context, the formation of unit 2 predates that of the perennial CO_2, whose age does not exceed a few centuries [*Thomas et al.*, 2005]. The age of unit 3 is more difficult to establish. We may however reasonably speculate that both units 2 and 3 were created during the same time frame. As discussed in section 2, the overall morphology of the terrains in these regions indicate substantial resurfacing by a potentially recent ice deposition event.

[5] There are at least two major questions associated with the presence of exposed perennial water ice at the south pole of Mars: (1) Is it currently in equilibrium? (2) Is the process responsible for its existence still active today? That the unit 2 area extends slightly beyond the limits of residual CO_2 is probably not a coincidence. The cold CO_2 ice surface helps stabilize the less volatile water ice substrate of unit 2 and thus may control its extent and equilibrium. Still, the origin of this unit cannot be explained by any scenario involving the residual CO_2 ice cap, since the latter is geologically younger. It is also difficult to explain its formation during the current climatic regime; Mars General Circulation Models (MGCMs) predict that perennial water ice at the south pole is unstable in the absence of residual CO_2 ice. This results from the current asymmetric pacing of seasons and the asymmetry of volatile transport between hemispheres [*Houben et al.*, 1997; *Richardson and Wilson*, 2002a]. One should therefore explore previous climatic regimes to find conditions conducive to the formation of unit 2 and, to a larger extent, that of unit 3.

[6] An obvious cause for climate change on Mars is the large, known variations in its orbit parameters [*Laskar et al.*, 2002, 2004]. These variations can significantly alter the phasing and distribution of solar insolation. While obliquity variations have received most of the attention [*Haberle et al.*, 2000; *Richardson and Wilson*, 2002a; *Mischna et al.*, 2003; *Haberle et al.*, 2003; *Levrard et al.*, 2004; *Newman et al.*, 2005], it is the precession cycle (i.e., the circular motion of Mars' rotation axis), modulated by eccentricity, that may control the relative size of volatile reservoirs in each hemisphere. In this paper, we attempt to explore the relationship between the water ice units identified by OMEGA and the climatic conditions arising from a seasonal shift of perihelion timing. We show that recent variations in the precession cycle may have been favorable for the deposition and stability of water ice at the south pole. We

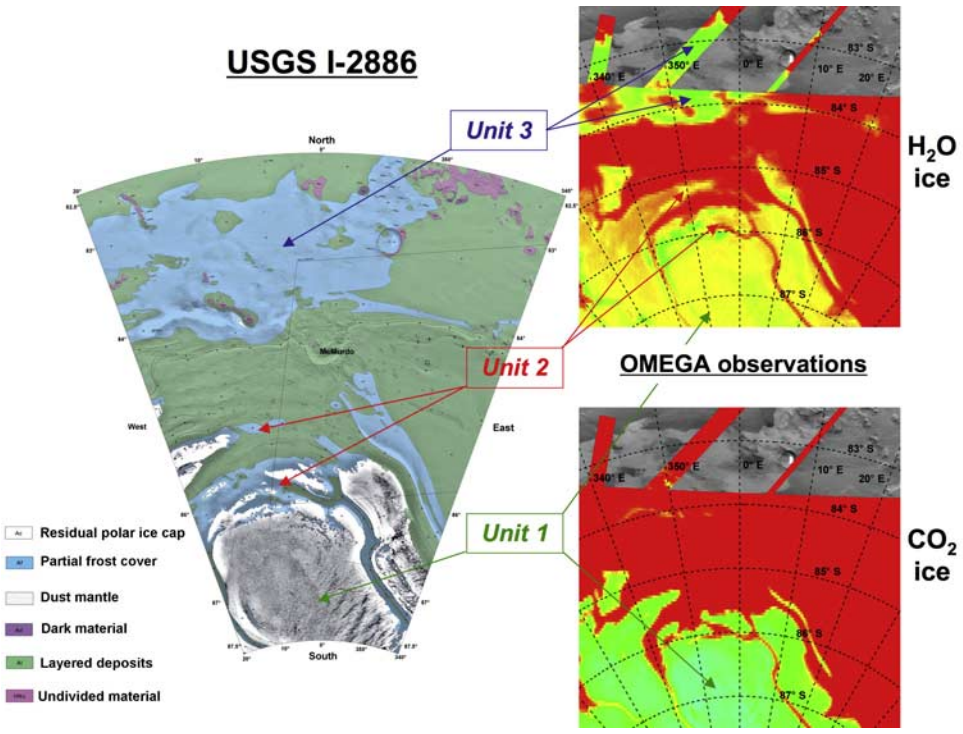

Figure 1. (left) Geological description of the south polar region extracted from the USGS I-2686 map. Color coding refers to the various geological units (indicated on the left) inventoried by K. Herkenhoff from Mariner 9 and Viking images. OMEGA observations of CO_2-free exposed water ice partly match the "partial frost cover" unit shown here as the light blue portions. The bright CO_2 ice cap is designated by the white/grey areas. Both units are surrounded by the millions year old polar layered terrains colored in green. (right) OMEGA mappings of (bottom) CO_2 ice and (top) H_2O ice in the same region. Images were obtained when Mars Express was 2160 km away from the surface yielding a resolution at pixel level of 2.7 km (except for the three diagonal tracks in the upper part which were obtained with a pixel resolution <0.5 km). Color coding indicates varying absorption levels for CO_2 and H_2O ices, going from red (0%) to green (60–70%). For H_2O ice, maximum absorption (in green) corresponds to a band depth level of 30% at 1.5 μm. For CO_2, maximum absorption is located in the bluish portion, corresponding to a band depth level of 40% at 1.435 μm. Images have been superimposed on Viking images (shown in grey). The locations of the various units defined by *Bibring et al.* [2004] and discussed in the text are shown here for clarity.

thus propose a scenario for the formation of units 2 and 3. To this end, we have employed a General Circulation Model of the Mars water cycle. First, we describe the OMEGA observations of the south pole in more detail. We then describe the model and present its results. Finally, we assess the viability of the proposed mechanism and discuss its sensitivity to other climatic variables.

2. South Polar Region

2.1. Brief Description

[7] To help the reader distinguish the major geological components of the south polar region, we display the USGS I-2886 map in Figure 1. The crater population of the south polar environment suggests a resurfacing age for its polar layered deposits (PLD) on the order of 10^7 years [*Plaut et al.*, 1988]. This is in stark contrast with those in the north polar environment which is effectively devoid of craters, indicative of a resurfacing age of about 10^5 years [*Herkenhoff and Plaut*, 2000]. Astronomical forcing has no preferred pole, hence an endogenous mechanism must be at work to produce such a hemispheric dichotomy of landforms.

[8] The permanent CO_2 cap, whose age has been recently reassessed using two consecutive years of monitoring by MGS/Mars Orbiter Camera (MOC) [*Thomas et al.*, 2005], stands apart within the 10 Ma old environment of the PLD. The CO_2 cap is comparatively very young (10^2–10^3 years), based on the measure of the scarp retreat and decaying rates of various erosional features, and appears to be composed of two distinct CO_2 ice units of comparable thicknesses (~5–10 m) which have been deposited some 100 years apart, a time interval during which the older unit degraded substantially [*Thomas et al.*, 2005]. Orbital timescales are greater than 10^4 years, so the presence of residual CO_2 cannot be explained by the classical Milankovitch theory.

[9] Modeling of the growth of the circular depressions (the Swiss cheese terrains) which are found all over the CO_2 cap shows that the observed geometry of the holes, with steep walls and flat floors, can only be produced by an active slab of retreating material (CO_2) overlying a less

active substrate, most likely H_2O [*Byrne and Ingersoll*, 2003]. The consensus that is now emerging is that CO_2 overlies a layer of water ice (i.e., unit 2). The latter can be observed at various locations around and across the cap [*Titus et al.*, 2003; *Bibring et al.*, 2004]. In addition, a distinct unit of water ice has been detected in the vicinity of the SRC [*Bibring et al.*, 2004]. It corresponds to isolated patches of <100 μm water icy grains with dust in various proportions. Unit 3, as defined by *Bibring et al.* [2004], was already identified in a previous geological inventory established from Viking images of the south polar region (USGS I-2886 map and legend). In this USGS map, unit Af, which was originally interpreted as a mixture of CO_2 frost and defrosted ground, encompasses units 2 and 3 since both exhibit a similar albedo, intermediate between that of the bright residual CO_2 ice cap and that of the darker polar layered terrains. Interestingly, part of unit 3 is observed to dip into a field of secondary craters associated with the McMurdo primary crater. In that area, the secondary craters appear more degraded. This may have been caused by relaxation of the craters due to flow of ground ice, or more likely due to deposition of water ice since the impact event (K. Herkenhoff, personal communication, 2006). This is an indication that water ice was emplaced after the formation of the PLD and that unit 3 cannot be the tip of an ice sheet buried deeper in the soil.

[10] While the age of these water ice units is difficult to estimate, their position in the layering sequence indicates that they are older than the upper CO_2 ice units (more than hundreds of years) and younger than the PLD (<10 Ma). This range is consistent with orbitally forced climate change as a mechanism to explain the origin of the water ice substrate. However, it is unlikely that these units could have formed under current climate. *Houben et al.* [1997] as well as *Richardson and Wilson* [2002a] report climate model experiments investigating the fate of a hypothetical water ice reservoir exposed at the south pole. In both experiments, the reservoir is rapidly exhausted, even if it is artificially forced with a summer surface temperature colder than that of the north polar cap. This suggests that units 2 and 3 cannot be created in the present climate regime. We speculate therefore that the age of the perennial water ice at the south pole is greater than the period of time during which current climatic conditions have prevailed, i.e., more than half the period of the fastest orbital cycle, the precession cycle (51,000 years), and is thus at least $\sim 10^4$ years old.

3. Past Climate Simulations

3.1. Previous Studies

[11] MGCMs have become useful tools for studying Mars' climatic response to known changes in its orbital parameters. Studies conducted to date have mostly focused on obliquity variations (the effect of tilting Mars' rotation axis to greater/smaller angles [*Haberle et al.*, 2000; *Richardson and Wilson*, 2002a; *Mischna et al.*, 2003; *Haberle et al.*, 2003; *Levrard et al.*, 2004]). These experiments have shown that equatorial reservoirs of ice may have been created during times of high obliquity. During the return to current, lower, obliquity, water was forced to migrate back to the poles, thereby creating the observed near-surface, ice-rich deposits at high latitudes [*Levrard et al.*, 2004]. However, a recent study has shown that the formation of dust lags during erosion periods, a process never accounted for so far, may drastically reduce the amount of water cycled in and out the polar regions [*Mischna and Richardson*, 2005].

[12] Less is known about how the water cycle responds to changes in eccentricity and precession, probably because they are second-order effects compared to obliquity variations. *Mischna et al.* [2003] have nonetheless simulated the Mars water cycle at high obliquity with various values of the argument of perihelion. While the model predicts that regions of water ice accumulation at high obliquity remain at low latitudes, changing perihelion causes the accumulation pattern to drift latitudinally about the equator. Precession and eccentricity force an asymmetry in the pacing of seasons and dictate which hemisphere is more likely to stabilize volatiles like water.

[13] *Jakosky et al.* [1993] have attempted to reconstruct the accumulation sequence of water ice at the north pole during the last 10^7 years on the basis of simple energy balance computations. They show that a thin layer of water ice is likely to exchange back and forth between the caps, the direction of such exchange being controlled by the argument of perihelion. However, the energy balance alone does not uniquely determine where ice will stabilize; atmospheric transport must also be considered since it controls moisture abundances and how they are distributed vertically and horizontally. MGCMs self-consistently resolve these processes and thus are better tools for studying surface ice accumulation process.

3.2. Cross-Equatorial Advection of Water

[14] Volatile transfer between hemispheres occurs via Hadley cells which are forced by differential heating across latitudes and which tend to reduce temperature contrast by moving hot air into cold regions. On Mars, topography makes this process highly asymmetric about the equator. The southern hemisphere is an elevated plateau which is 2 or 3 km higher than the northern plains. This difference in elevation influences the meridional wind pattern. Circulation models indicate that the southern summer Hadley cell is many times stronger than its northern summer counterpart whose flow overturns in the opposite direction [*Richardson and Wilson*, 2002b]. This bias is independent of any orbital factor (i.e., eccentricity/perihelion argument) and has acted since the formation of the north-to-south topographic dichotomy. Alone, the topographic forcing of the circulation favors the accumulation of volatiles in the northern hemisphere, hence the deposition of water and dust at the surface of the north polar region. If enhanced accumulation leads to a more effective resurfacing process, then this asymmetric transport process may have contributed to the 2 orders of magnitude difference in resurfacing ages of the northern and southern PLD (100 ka versus 10 Ma [*Herkenhoff and Plaut*, 2000]). This topographic bias led *Richardson and Wilson* [2002b, p. 300] to speculate that "a southern water ice cap occurs with a period of $>10^6$ years rather than the $\sim 10^5$ years predicted if one considers only cyclic variation in solar heating driven by precession." In other words, recent ($<10^6$ years) orbital variations have not provided favorable

combinations of precession/eccentricity/obliquity to allow water accumulate near the south pole.

[15] However, there are other factors that contribute to the net meridional transport of water. One factor particularly important concerns the altitude of cloud formation and the coupling of winds with cloud sedimentation. This factor was first described by *Clancy et al.* [1996] and was studied later with MGCMs for the current Mars climate [*Richardson et al.*, 2002; *Montmessin et al.*, 2004a]. Although the Hadley circulation is always strongest during southern summer, the movement of water between hemispheres depends more critically on the altitude of the hygropause (level of water vapor saturation) with respect to the depth of the Hadley cell. The hygropause is a direct result of adiabatic cooling of rising air masses in the tropical upwelling zone. During northern spring/summer, which presently occurs near aphelion, the upward motion and subsequent adiabatic cooling is reinforced by the reduced solar input such that water vapor saturates, condenses and precipitates before it can reach the upper horizontal branch of the Hadley cell and be carried southward. This large-scale condensation process has observable consequences since it produces the well-known ''aphelion cloud belt,'' a ring of clouds encircling the northern low latitudes [*Clancy et al.*, 1996]. The same does not currently occur during southern summer since the warmer perihelion climate pushes the hygropause to sufficiently high altitudes that cloud formation is subdued in the southern summer tropics and water is able to move freely to the north.

[16] *Clancy et al.* [1996] applied these principles, which we refer to as the ''Clancy effect,'' to extrapolate their impact when averaged over the precession cycle: When water sublimates from the pole whose summer coincides with the colder conditions of aphelion, water is forced to pool in this same hemisphere as a result of cloud-induced sequestration in the tropical convergence zone of aphelion. Dust particles, which likely serve as cloud condensation nuclei, should be similarly confined through scavenging processes. Thus the Clancy effect may be regarded as an equatorial valve that regulates the net meridional transport of dust and water depending on the difference in thermal environments between northern and southern summer. Under current orbital configuration, the colder near-aphelion northern summer and the topographic circulation bias each act to favor the accumulation of water (and probably dust) in the northern hemisphere.

[17] With the argument of perihelion shifted to northern summer, a configuration which prevailed half a precession cycle ago (−25,000 years), the Clancy effect would favor sequestration of water in the southern hemisphere, but the topographic circulation bias would still favor the northern hemisphere. Without detailed studies with an MGCM, it is not possible to determine a priori which hemisphere is favored for ice accumulation and therefore whether or not water was transferred to the south pole less than 1 Ma ago. Answering this question is the goal of this paper.

3.3. Model Description and Simulation Settings

[18] We use MGCMs developed at the Laboratoire de Météorologie Dynamique (LMD) [*Forget et al.*, 1999] and at NASA Ames Research Center [*Haberle et al.*, 1999]. We first use the LMD model with a resolution of 5.625° in longitude and 3.75° in latitude. This model has been recently modified to reproduce the present-day water cycle and is in good agreement with MGS/Thermal Emission Spectrometer (TES) observations [*Montmessin et al.*, 2004a]. Water is exchanged between the atmosphere and the surface, is transported by winds, and condenses to form clouds when saturation conditions dictate. The cloud scheme uses a simplified microphysical treatment based on a prescribed number of available condensation nuclei that varies linearly with the column dust opacity. Despite the relative crudeness of the cloud scheme, it allows the cloud particle radius to change as a function of the predicted mass of condensation. This is a small but substantial step forward when compared with other models where cloud particle size remains constant at present-day values [*Richardson and Wilson*, 2002a; *Mischna et al.*, 2003]. As shown by past climate simulations using the LMD model, cloud particles can potentially reach sizes 10 times larger (20–50 μm) than their current value [*Forget et al.*, 2006]. A tenfold increase of particle radius intensifies water precipitation by at least the same factor (settling velocity is proportional to particle radius but may vary as the square of the radius near the surface where the atmosphere is denser) and subsequently affects surface water ice budgets [*Forget et al.*, 2006]. In our model, clouds are radiatively inactive, but we represent the alteration of surface properties by setting the albedo to 0.4 whenever deposition of water ice exceeds 5 μm in thickness.

[19] Our goal is to address the impact of precession on the Mars water cycle and to determine if this cycle may have allowed water to accumulate in the south polar region in the recent past. To this end, we have chosen to run MGCM simulations using the orbital configuration that prevailed 21,500 years ago and which corresponds to the last time perihelion occurred during northern summer. We refer these simulations to as ''reversed perihelion'' simulations to indicate they are a mirror image of the current orbital configuration. We chose this date because it represents a time when the contrast in summertime insolation between the poles is maximized (as shown in Figure 2, this difference was around 70 W m^{-2}) and the Clancy effect favored the southern hemisphere for water accumulation. As computed by *Laskar et al.* [2004], orbital parameters prevailing 21,500 years ago were defined by an obliquity equal to 23.45°, an eccentricity of 0.0761, and an areocentric longitude of perihelion (Lp) of 99°.

[20] Dust is a critical climatic variable since it controls the thermal structure of the atmosphere. It is obviously also critical for cloud formation since condensation depends nonlinearly on temperature. The current dust cycle exhibits a pronounced peak in opacity during southern summer [*Smith*, 2004], reinforcing atmospheric warming associated with the increase of solar input of perihelion. For this reason, no large-scale cloud formation similar to that of aphelion is observed to occur in the tropics near perihelion. Because the Clancy Effect is sensitive to atmospheric temperatures, the representation of dust radiative forcing requires careful consideration. *Newman et al.* [2005] have studied the dust cycle response to limited orbital variations. In particular, they predict an amplitude reduction of the seasonal dust cycle in the case of reversed perihelion, and also that perihelion remains the season with higher lifting.

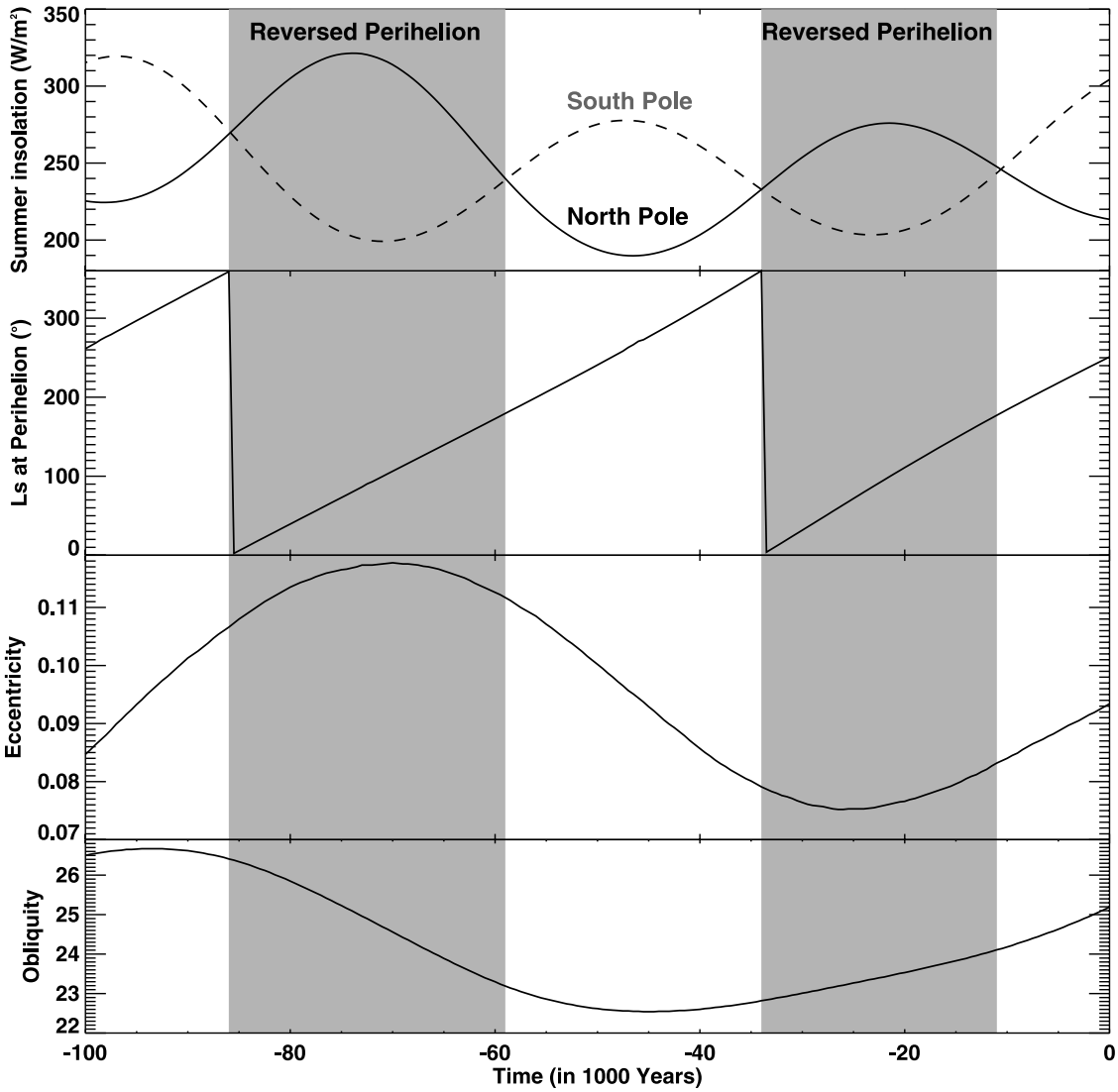

Figure 2. Variations of summer insolation at both poles and corresponding variations of the orbital parameters during the last 100 ka. The reversed perihelion regimes, shown here as the shaded grey portions, bracket periods when the areocentric longitude of perihelion argument (Lp) is greater than 0° and smaller than 180°. The shortest modulations of insolations track the secular changes of Lp. A longer-term increase of insolation contrast between the poles is also noted; it is associated with the increase of eccentricity between −20 and −70 ka.

We shall discuss later similar results obtained with the NASA Ames MGCM. On this basis, we have investigated several scenarios in order to bracket the Mars water cycle response to a variety of dust cycles in a reversed perihelion situation:

[21] 1. The first scenario is referred to as "constant dust" (CD) scenario. Here the visible dust opacity (τ) is held constant at a value of 0.2. The vertical distribution is represented by a Conrath-like formula [see *Forget et al.*, 1999] with a dust top located around 40 km.

[22] 2. The second scenario, the "dusty perihelion" (DP) scenario, is a transposition of the dust opacity cycle described by *Montmessin et al.* [2004a] and used by our MGCM to simulate present-day conditions. The time and space arguments of these ad hoc prescriptions of opacity and vertical distribution have been symmetrically adjusted to make northern summer the dustiest season of the year ($\tau > 0.5$) and southern summer the clearest ($\tau \sim 0.1$). This mimics, though somewhat exaggerates, the results of *Newman et al.* [2005].

[23] 3. A third scenario, the "dusty aphelion" (DA) scenario, uses the present-day prescription, i.e., the dustiest (clearest) time of year occurs during northern winter (summer). The assumption here is that perihelion argument has no impact on the dust cycle.

3.4. CO_2 Cold Trap

[24] The coexistence of H_2O and CO_2 ices at the surface of the central portion of the SRC is due to a cold-trapping process. This accumulation of water implies that some other reservoir is losing water. The latter can be the regolith, the north residual cap or the recently discovered water ice units

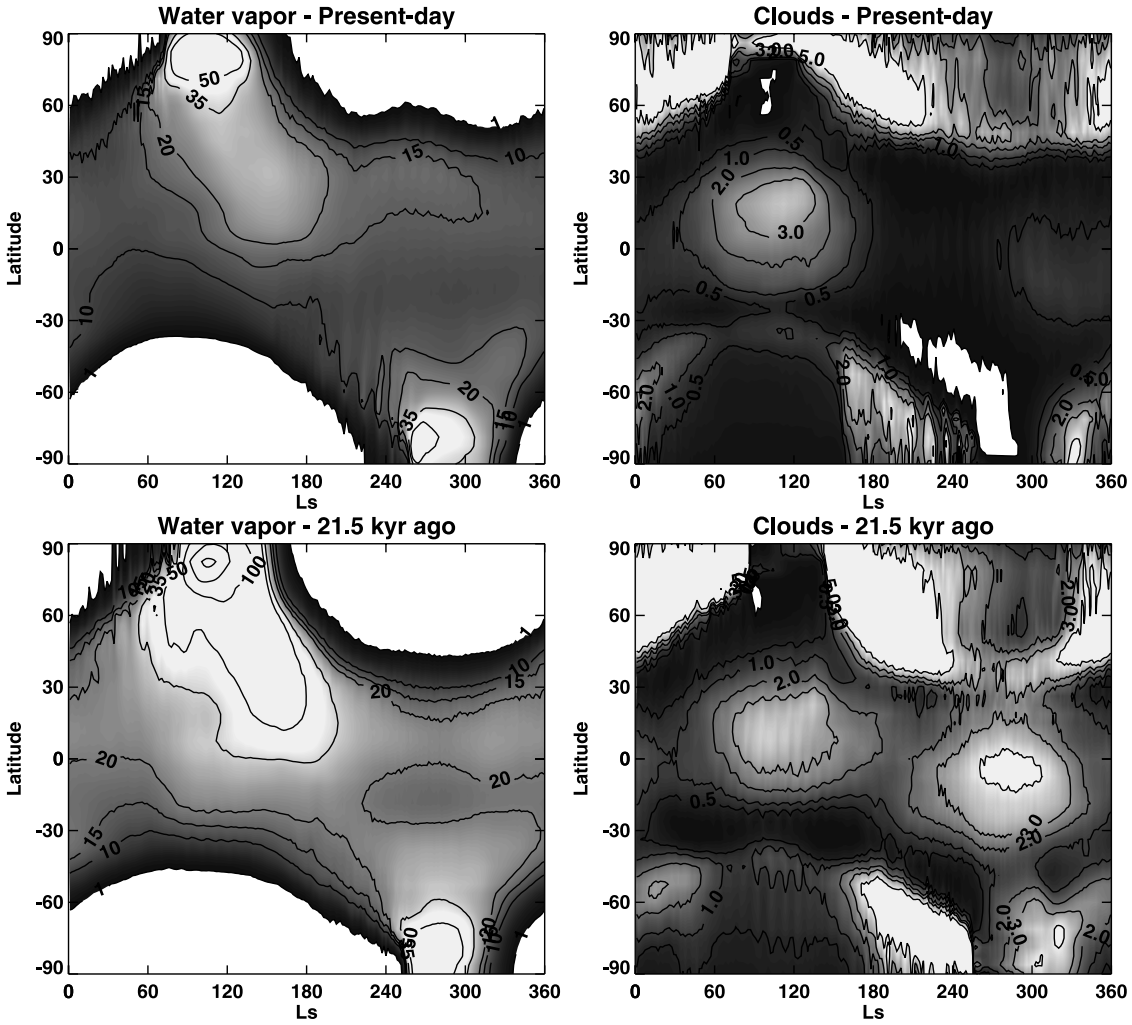

Figure 3. Seasonal and latitudinal distribution of (left) water vapor and (right) water ice clouds for (top) current and (bottom) reversed perihelion configurations. Quantities are expressed in pr μm.

of the south pole. Previous modeling efforts indicate that the amount of water captured by residual CO_2 corresponds to a layer of about 50 μm potentially extracted each year from the north polar cap [*Houben et al.*, 1997; *Richardson and Wilson*, 2002a; *Montmessin et al.*, 2005]. However, the CO_2 cold trap, which has a moderate impact on today's water cycle, cannot be considered as a permanent component of the system since it forms and vanishes with a timescale supposedly shorter than the ones investigated here. For this reason, all the reversed perihelion simulations have no CO_2 cold trap at the south pole. In addition to being unrepresentative of a reversed perihelion situation, the presence of a CO_2 cold trap would also force a net transfer of water from north to south. Since our goal is to determine if precession and the Clancy Effect can overcome the topographic circulation bias, removing the cold trap eliminates the ambiguities its presence would introduce.

3.5. Reversed Perihelion Simulations

[25] In this section, we limit our discussion to the CD simulation and compare it with a simulation of the present-day water cycle. The orbital configuration that reigned 21,500 years ago imposed that the north pole received 35% more summertime insolation than the south pole did and 30% more than it does today. In theory, peak temperatures at the surface of the north residual cap should have been raised by about 20 K (222 K for present-day versus 240 K for the −21,500 year simulation), resulting in sublimation rates 2 to 3 times greater: 200 precipitable (pr) μm of column-integrated water vapor over the north polar region are obtained for the −21,500 year case compared to 75 pr μm (see Figure 3) for present-day, the latter value being consistent with MGS TES observations [*Smith*, 2002].

[26] Figure 4 indicates that in a reversed perihelion climate, the southern hemisphere gains water at all seasons while the northern hemisphere experiences higher water abundances only during spring and summer. Figure 3 (bottom left) indicates that there is a pronounced increase in the water column at high southern summer latitudes in the reversed perihelion simulation despite the phasing of southern summer with aphelion. This increase is initially drawn from the higher water abundance of the northern low latitudes during northern summer through the solstitial overturning circulation. This extra amount of water then condenses and accumulates as frost in mid-to-high southern

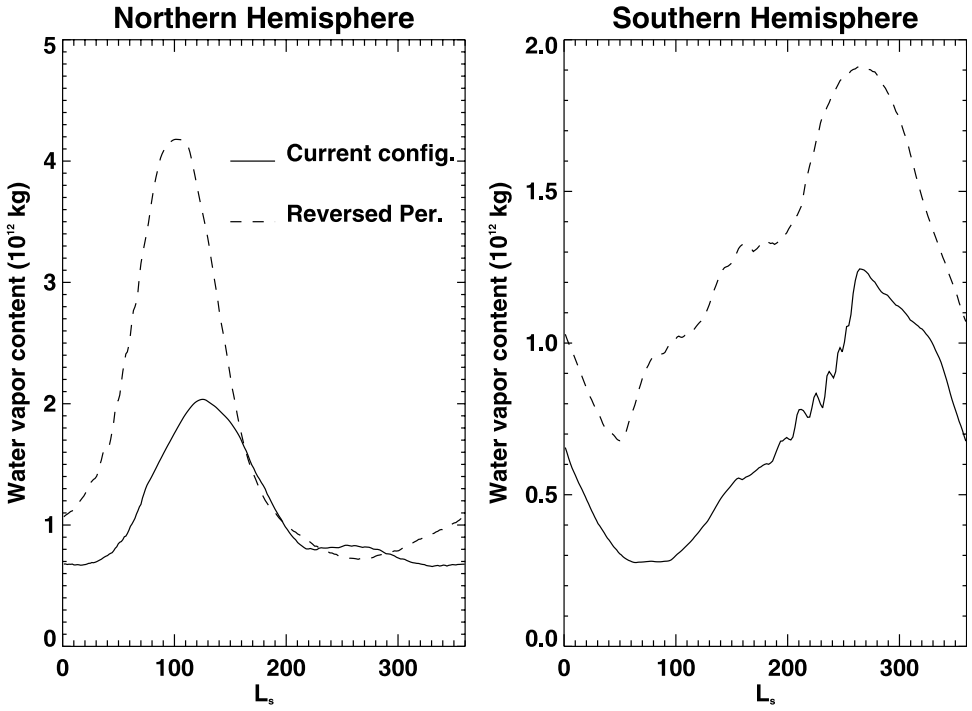

Figure 4. Seasonal variations of integrated water vapor content in each hemisphere for the two opposite perihelion configurations simulated with the model. Increased summer insolation results in a twofold enhancement of the northern water content for the reversed perihelion case. Both simulations fluctuate around a similar level of humidity in fall and start to deviate again after Ls 300°. Southern hemisphere exhibits an annually wetter state compared to present-day simulation.

winter latitudes and is later released during the following southern spring/summer. Cloud patterns exhibit a similar pattern in both simulations. The only major differences noted in the reversed perihelion simulation are the presence of a cloud belt in the summer low latitudes of the southern hemisphere and a more opaque polar hood accompanying the retreat of the seasonal CO_2 frost in the south.

[27] As shown in Figure 5, today's configuration results in the formation of unit 1 (according to OMEGA classification), i.e., water ice trapped within the south residual cap. The effect of a CO_2 cold trap at the south pole is modeled by forcing the surface temperature to be at the vapor-ice transition temperature of CO_2 ($\sim$140 K). The model predicts an annual accumulation of 400 μm of water ice over the residual CO_2 cap but no accumulation beyond the cap limits. In the reversed perihelion simulation, the absence of a CO_2 cold trap does not prevent water ice deposition. On the contrary, we find that a water ice layer permanently mantles the polar region at every longitude south of 80°S. The cover extends slightly beyond 80°S and reaches the 75°S contour, but the water ice deposition pattern is much more structured in this zone. The layer thickens at a rate of 500 μm yr^{-1} and up to 1 mm yr^{-1} in a small area located south of the 85°S annulus close to the Prime Meridian. The total mass of ice accumulating every year in the south polar region is equivalent to about half the total inventory of water vapor in the southern hemisphere, i.e., 0.5 Gt.

[28] If one assumes that a value of 500 μm yr^{-1} corresponds to the maximum accumulation rate of water ice near the south pole during the reversed perihelion part of the last precession cycle (i.e., $0° < Lp < 180°$), that no accumulation occurs at the limits of this 25,000-year timeframe, and that accumulation rate evolves linearly with time, then a >6-m-thick layer could have formed near the south pole during the last excursion of perihelion argument in northern spring and summer.

3.6. Sensitivity to Dust

[29] Potential climatic feedbacks (e.g., dust and cloud radiative effects) are difficult to assess in the context of a reversed perihelion situation and more generally in the context of any orbital change. Dust, in particular, has a profound impact on the hygropause altitude and thus can potentially alter the meridional transport of water. Figure 6 is a good illustration of how changing the dust cycle can lead to different water transport patterns. The dusty perihelion (DP) scenario has a substantial increase of dust opacity during northern summer. Compared to the other scenarios, where the dust opacity is constant at a low value (CD case) or forced to peak during the opposite southern summer season (DA case), water vapor in the DP scenario spreads both vertically and horizontally during northern summer, as shown by the elevated and expanded contours in Figure 6. The dustier and subsequently warmer atmosphere of DP possesses a higher holding capacity and is therefore able to extract additional quantities of water off the subliming north polar cap. In the CD and DA scenarios, the north polar atmosphere saturates at low levels in summer, leading to cloud formation and water confinement near the surface. In the DP case however, the atmosphere remains below

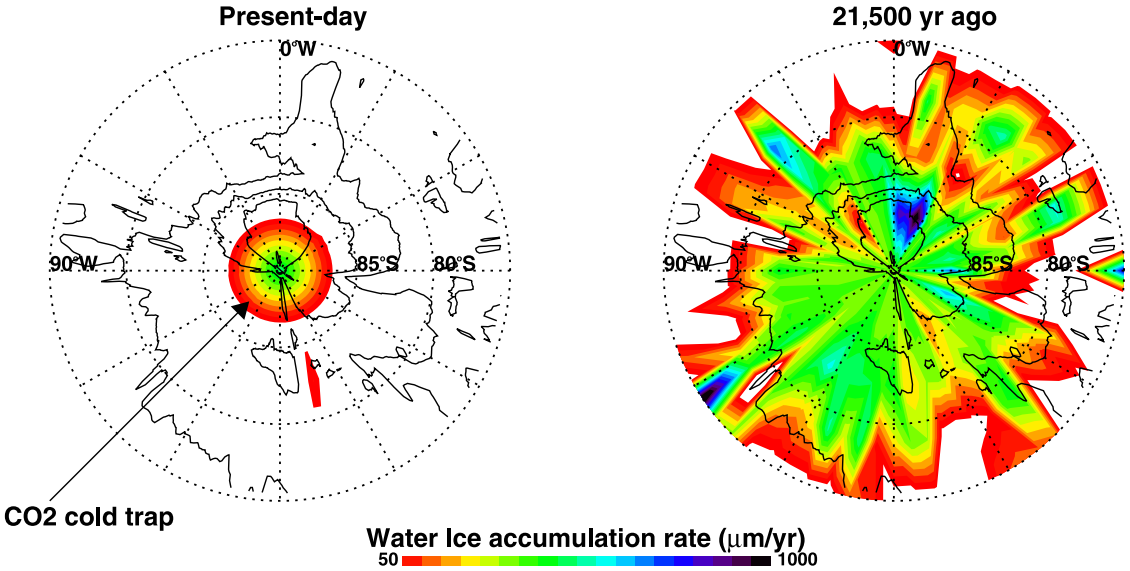

Figure 5. A comparison of water ice accumulation rates predicted by the model in the south polar region for the two perihelion configurations. Present-day map shows net accumulation only at the south pole itself (equivalent to 1 grid point in the model) where the prescription of a CO_2 cold trap forces a local and permanent deposition of water ice. In the reversed perihelion simulation (Figure 5, right), the CO_2 cold trap has been removed and the pattern of accumulation is only controlled by a precipitation versus sublimation positive balance on an annual average.

saturation and water is carried equatorward without cloud limitations.

[30] In the low to midlatitudes where the rising branch of the Hadley cell is located, the higher dust loading of the DP scenario forces the condensation level to be moved more than one scale height upward. Because saturation intersects a more elevated portion of the Hadley cell, condensation and subsequent confinement by sedimentation does not affect the bulk of water vapor that follows cross-equatorial streamlines at lower heights. The higher dust content of the DP simulation also impacts circulation strength, as originally explained by *Haberle et al.* [1982]. The strength of the Hadley circulation is known to respond quasi-linearly to increasing dust content due to the amplification of the latitudinal temperature gradient. Figure 6 shows that the Hadley cell is more developed in the DP simulation. In such conditions, the higher condensation level couples with a faster stream to facilitate and intensify water advection to the south.

[31] The net annual exchange of water between hemispheres depends on how transport during northern summer is balanced by transport during southern summer. This exchange is determined primarily during these two seasons since around equinoxes, the Hadley cell reverses and the circulation is much weaker. Figure 6 shows that during southern summer in all the reversed perihelion simulations, water vapor is confined to a shallow layer, especially in the DP case which has the smallest amount of dust at this season. In all three cases, the colder conditions of aphelion limit extraction of water from the south polar region by keeping water from using the full depth of the Hadley cell for northward advection. Consequently, water remains locked in the southern hemisphere.

[32] Because the dust opacity in the DP scenario is in phase with the seasonal variations of insolation, it produces the strongest seasonal temperature contrast, and therefore amplifies the strength of the equatorial water valve and leads to a greater accumulation of water ice in the southern hemisphere. Figure 7 shows, indeed, that the net annual accumulation of water ice in the southern hemisphere is a factor of 4 greater than in the CD scenario, and a factor of 6 greater than in the DA scenario. This difference between scenarios can be essentially attributed to the Clancy effect, which thus appears able to modulate water transport by nearly 1 order of magnitude. The fact that water accumulates at the south pole in all three cases demonstrates that the north-to-south transfer of water is robust to the uncertainties on dust loading variations with precession cycle.

3.7. Stability of a South Polar Mantle Under Current Climate

[33] In order to determine the fate of the south polar water ice mantle that is predicted to have formed during the "reversed" part of the precession cycle, we have run two additional simulations with orbital parameters set to present-day values. We did not include a CO_2 cold trap at the pole in order to focus solely on the orbital influence on the stability of ice. Two sources of water are set: (1) the north polar cap and (2) the south polar mantle, represented by a surface reservoir of ice south of 80°S for one simulation and south of 85°S for the other. According to previous studies [*Richardson and Wilson*, 2002a; *Houben et al.*, 1997], such austral reservoirs should be unstable with respect to current climate forcing, and we expected to draw a similar conclusion with our model. However, these simulations were intended to further investigate the potential mode of recession of this polar ice mantle, so as to track its successive

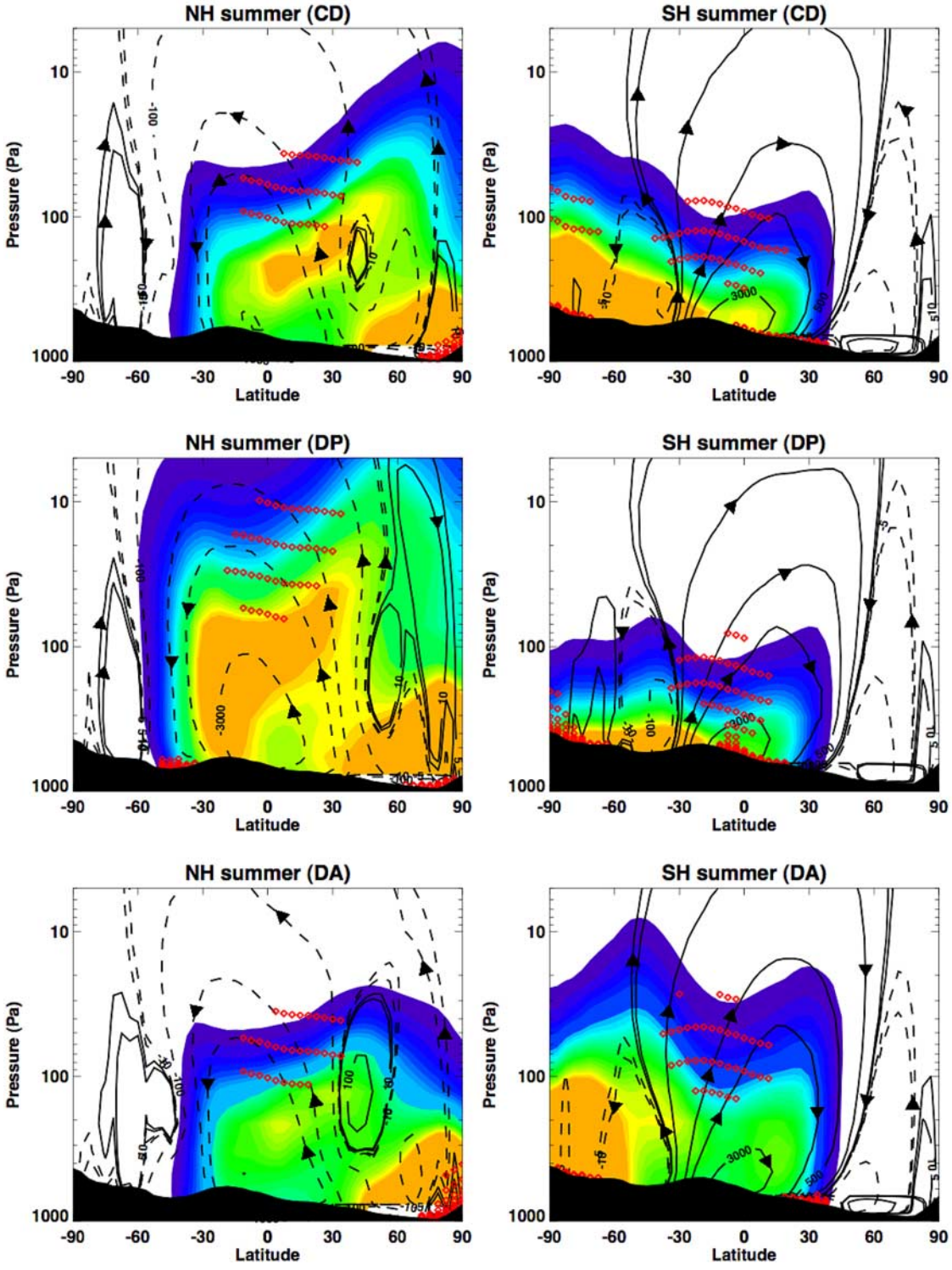

Figure 6. Meridional cross section water advection patterns simulated for the reversed perihelion configuration. Three dust scenarios are investigated (top to bottom). (left) Northern and (right) southern summer seasons are shown. Color contours are coded according to water vapor concentrations (purple ~1 ppm to orange ~250 ppm). Streamlines are indicated by solid and dashed lines; values refer to the stream intensity ($\times 10^6$ kg s^{-1}). Red diamonds indicate the presence of water ice clouds.

stages of recession. Considering the significant thickness of the icy mantle, we have set its surface thermophysical properties to be consistent with an icy substrate (thermal inertia set to 1000 SI, and albedo to 0.4). These higher albedo and thermal inertia values, compared to those of a bare soil, multiply survival chances for surface ice. Still, they do not warrant its stability. In Figure 8, we map the water ice erosion rate (μm yr^{-1}) predicted by the model in

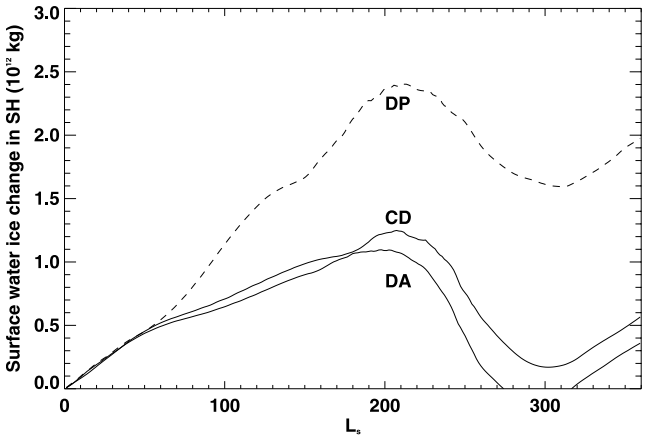

Figure 7. Seasonal variation of total surface water ice south of the equator in a reversed perihelion configuration for the three dust opacity scenarios discussed in section 3.6. The dusty perihelion (DP) scenario yields the largest net deposition of water, with an enhancement factor of 4 and 6, respectively, compared to constant dust (CD) and dusty aphelion (DA) simulations. Variations track each other until approximately Ls 50°, after which date, changes in water transfer from the northern hemisphere become apparent between simulations. The warmer northern tropics of the DP scenario allow additional amounts of water to move south and to condense there. Around Ls 200°, the DA simulation produces the strongest atmospheric warming, and subsequently allows more water return to the northern hemisphere.

the south polar region for the two different simulations. As expected, ice no longer remains there with perihelion phased with southern spring/summer and returns to the north pole where conditions are more favorable. In the case where the reservoir is located south of 80°S, the erosion pattern depicts a nearly concentric annulus almost devoid of longitudinal structure. Closer to the pole, the region remains preserved from ablation except for a portion located in the [60°W, 30°E] sector where a peak of erosion is predicted to extend from the pole up to 80°S. In the other simulation, supposed to represent a later stage of recession where the southernmost boundary of the ice mantle is located at 85°S, a similar concentric erosion pattern is found. With rates up to a few millimeters per year, the survival time for the meters-thick icy mantle should be of about 10^3–10^4 years, i.e., of the order of, or less than, the precession timescale. Our results are in line with previous studies and confirm that in the absence of a CO_2 cold trap, water ice is not perennial at the south pole under current climate. The model further suggests that water ice deposited during one phase of the precession cycle can potentially be removed during the opposite phase, thereby creating a precession-induced exchange of water between the poles.

4. Discussion

4.1. A Scenario for the Formation of the Water Ice Units

[34] Elaborating upon model results, we may envision a scenario for the origin of the perennial water ice units observed by OMEGA in the south polar region. There is no clear geological signal for the age of these units. As discussed previously, they likely formed before the permanent CO_2 ice sheet (10^2 years) and after the PLD terrains (10^7 years). The fact that observed water ice boundaries exhibit striking conformity with those of the CO_2 cap, except for the isolated units that lie slightly farther equatorward, suggests there is a process linking the areal extent of the cap to that of the water ice units. Here, we suggest the following sequence of events to explain these observations:

[35] 1. During the reversed perihelion regime, which lasted ~25,000 years between −34,000 years and −10,500 years, insolation and transport conditions were

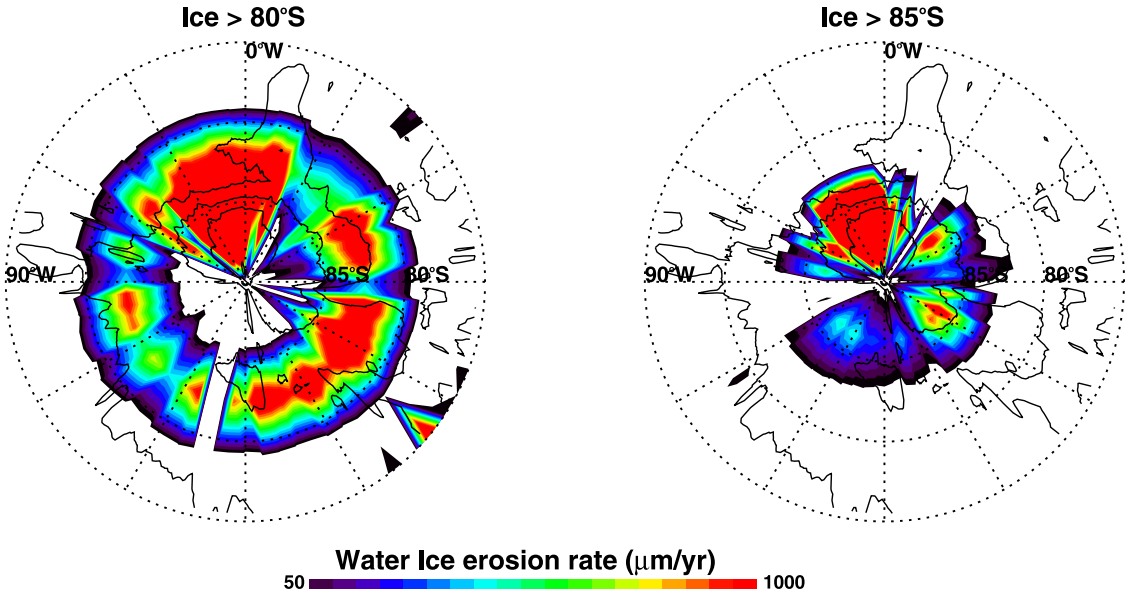

Figure 8. Annual erosion rate of a hypothetic water ice mantle located (left) south of 80°S and (right) south of 85°S predicted by the model under current climatic configuration.

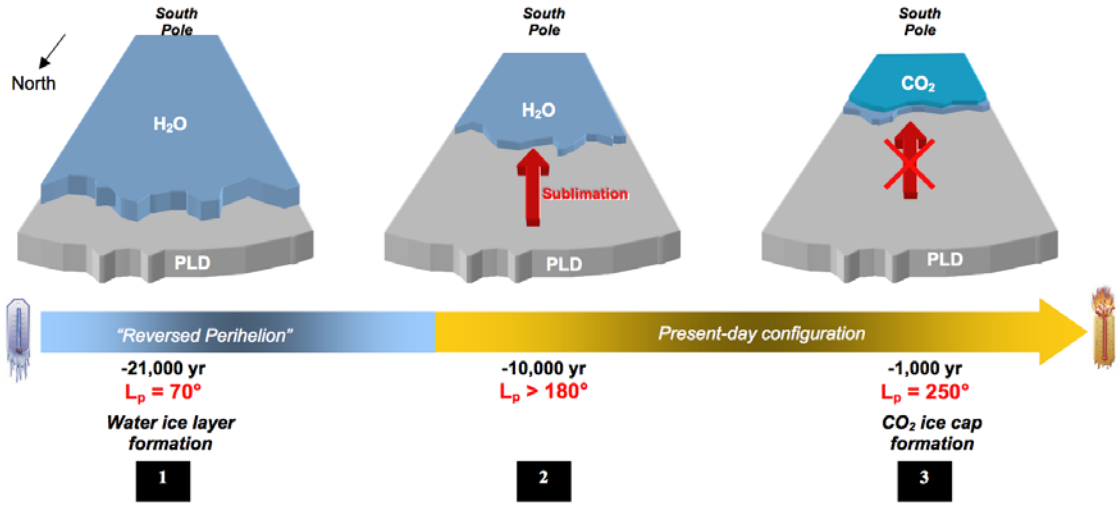

Figure 9. Illustration summarizing the sequence of events in the south polar region since the last reversed perihelion regime of the precession cycle. At event 1 time, water was extracted off the north polar cap and was deposited over the south PLD terrains thanks to a favorable summer insolation gradient between the poles. For event 2, passage to present-day configuration, with perihelion argument now entering a northern spring regime, reversed the orientation of the insolation gradient and forced water to progressively return back to the north pole. For event 3, in a third act, the erosion process stopped as permanent CO_2 ice slabs formed and kept water from subliming further.

such that water ice was extracted from the north polar cap and accumulated near the south pole. This eventually formed a circumpolar mantle which extended to approximately 75°S (i.e., far beyond the current boundaries of the units) and reached several meters in thickness.

[36] 2. At 10,500 years ago, perihelion argument shifted into present southern spring/summer regime, reversing the north-to-south gradient of insolation between the poles. Following this change, perennial water ice became unstable at the south pole and started to return to the north.

[37] 3. With increasing southern summer insolation, sublimation intensified and the water ice mantle progressively receded poleward.

[38] 4. Some 10^3 years ago (according to estimates on the age of residual CO_2), some unknown process triggered the formation of permanent CO_2 ice slabs over the receding water ice layer. The presence of CO_2 ice imposes temperatures far below the condensation point of water vapor and thus creates a cold zone that maintains the stability of water ice at latitudes where it would otherwise be removed by sublimation. The formation of the permanent CO_2 subsequently protected water ice from further erosion.

[39] A sketch of these events is displayed in Figure 9. According to this scenario, the water ice units mapped by OMEGA outside the CO_2 cap are the remnants of >10,000 years old deposition events. In the absence of permanent CO_2 ice, these water ice units would have probably disappeared and no water ice would now be exposed. The presence of outliers (unit 3) is not well explained by the above scenario. However, they might reflect preferred deposition zones. The model predicts some structures in the accumulation pattern, with significant enhancement in a small area of the western hemisphere located just south of one of the two isolated units discovered by OMEGA. Even though these observed patches are not geographically connected to the SRC, they might be close enough to have their erosion reduced by some mesoscale stationary cold flow forced locally by the CO_2 cap. In fact, a similar pattern of perennial water ice distribution is observed in the north residual cap, with elongated patches lying a few degrees south of the main circular unit.

4.2. A Precession Signal in Martian Geological Records?

[40] The proposed explanation for the origin of perennial water ice at the south pole is based on a precession-controlled mobilization of water between the poles. This mechanism may only operate at low obliquity (<35°) when insolation distribution favors storage of water in the polar regions whereas higher obliquities force accumulation to concentrate near the equator [*Richardson and Wilson*, 2002a; *Mischna et al.*, 2003; *Levrard et al.*, 2004; *Forget et al.*, 2006]. Hence the precession cycle should have affected the geology of the north polar region and the analysis of the north PLD stratigraphy suggests that it did. Extending the technique used by *Laskar et al.* [2002] to extract climatic signals from a sequence of layers exposed in a vertical section of the north polar cap, *Milkovich and Head* [2005] have confirmed that the first 350 m of the cap can be associated with the insolation variations of the last 0.5×10^6 years. Since this orbital timeframe was mostly dominated by the fundamental 51 ka period of precession, each of the 30-m layers is interpreted as the result of the changing style of water and dust deposition during each precession cycle.

[41] The south polar region has not experienced a comparable accumulation of layers. Analysis of the cratering pattern indicates that not more than 10 m of material have been deposited during the last 10^6 years [*Plaut et al.*, 1988; *Herkenhoff and Plaut*, 2000]. A thin layer similar to that

predicted by the model (<10 m in thickness) may thus have exchanged several times between the caps during this period, while the associated resurfacing has been too moderate to leave visible marks on the surface. This further implies that every time water has been deposited in the south during the northern spring/summer phase of the precession cycle, it has totally sublimated during the following southern spring/summer phase. Otherwise a stack of layers would have progressively formed and would now be observed like in the north. This also means that a residual dust lag capable of shutting down the sublimation of the water ice sheet has not developed in the south polar region as it is thought to have developed in the north.

[42] However, this brings up the following conundrum: if only a thin layer (<10 m) has exchanged between the poles on Mars during the last precession-dominated 0.5×10^6 years, then how could more than 300 m of material have accumulated over the north polar cap? This requires an additional exchangeable water reservoir in order to allow the north polar cap build up such thicknesses. This may be explained by exchanges with a tropical ice reservoir formed at times of high obliquity [*Levrard et al.*, 2004]. Near subsurface water ice, as observed by Mars Odyssey [*Boynton et al.*, 2002], is also a good candidate since it can diffuse through the regolith on timescales much shorter than the precession cycle [*Mellon and Jakosky*, 1993]. Further investigations coupling a regolith and climate model will be needed to help elucidate this question.

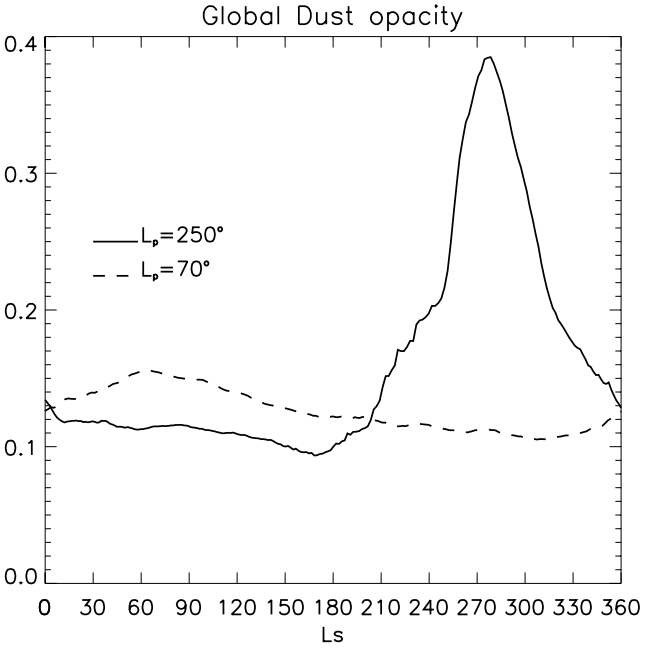

Figure 10. Dust cycle predicted by the Ames GCM for present-day (solid curve, Lp = 250°) and for a reversed perihelion case (dashed curve, Lp = 70°). Opacity is given at a wavelength of 9 μm (a multiplicative factor of ~2 must be applied to obtain corresponding visible opacity).

4.3. A North/South Differentiation Mechanism

[43] The difference in polar environments is thought to result from their difference in elevations, which alters the meridional transport pattern and the stability conditions of volatiles at the surface. Here, we propose an additional mechanism favoring the north-to-south differentiation. Various climate models predict that precessional variations should modulate the seasonal variation of dust lifting, in particular the perihelion-to-aphelion amplitude [*Haberle et al.*, 2003, *Montmessin et al.*, 2004b; *Newman et al.*, 2005]. The results of *Montmessin et al.* [2004b] and *Haberle et al.* [2006] were obtained by the MGCM developed at NASA Ames and described in detail by *Haberle et al.* [1999] and *Kahre et al.* [2006]. This model runs in a so-called "interactive dust" configuration, where dust is lifted by dust devils and large-scale winds using representations described by *Newman et al.* [2002] and *Kahre et al.* [2006]. Particles are advected by circulation and interact with the radiation field. The lifting parameters were tuned so as to produce a dust opacity cycle consistent with observations, i.e., a clear atmosphere ($\tau_{IR} \sim 0.1$) during northern spring summer and an increase in opacity during southern spring ($\tau_{IR} \sim 0.5$). The model was then run with the argument of perihelion shifted to Lp ~ 70° (which is the same value as *Newman et al.* [2005] and is very close to the 99° employed for the water cycle simulation), but keeping the modern day lifting parameters. The results are plotted in Figure 10 and show both the modern dust cycle (Lp ~ 250°) and the reversed perihelion dust cycle (Lp ~ 70°). The annual evolution predicted for the reversed perihelion situation is marked by a significant reduction of the perihelion-to-aphelion opacity amplitude. As was found by *Newman et al.* [2005], the perihelion season remains the dustiest season of the year, which suggests that lifting is controlled first by insolation variations. This difference of lifting patterns between the two orbital configurations is essentially due to the absence in the northern hemisphere of regional sources as productive as the Hellas basin.

[44] In theory, therefore the flat dust cycle of reversed perihelion cannot amplify thermal contrast between aphelion and perihelion like it does under current climate. The implications for the migration of water between the poles can be inferred from the results of section 4.2. The NASA Ames and LMD/Oxford MGCMs suggests that a reversed perihelion dust cycle is closer in behavior to the CD case, whereas the current perihelion setting is rather akin to the DP case (i.e., a significantly dustier perihelion season), the latter producing factor of four greater accumulation rates in the polar region. This implies that the north-to-south transfer of water under a northern spring/summer regime of the perihelion argument is curtailed by a factor of 4 from its full potential, whereas the opposite south-to-north transfer occurring during the other part of the precession cycle operates at nearly full capacity.

5. Conclusion

[45] This study suggests that the most recent precession cycle (<10^5 years) is responsible for the origin of the majority of the water ice observed at the south pole. It further suggests that precession and the Clancy Effect can drive a net north-to-south transfer of water, thereby overcoming the "north handed" topographic bias of the circulation. Our climate model shows that a shift of the

perihelion argument from its current position (Lp = 250°) to one 180° later (Lp = 70°) results in the accumulation of water ice in the south polar region, building a meters-thick circumpolar mantle of ice when integrated over half a precession cycle. With these results, we propose an explanation for the origin of the perennial water ice units of the south pole whose existence has been inferred from observations by the MGS and Mars Odyssey missions and which have been mapped and further characterized by OMEGA on Mars Express. The perihelion configuration of the last 10^4 years has destabilized water at the south pole, and this has forced the water ice mantle formed during the previous reversed perihelion period to recede poleward. Recently, however, the formation of the permanent CO_2 ice cap on top of the decaying mantle has ''frozen'' water ice in its current eroded state.

[46] On this basis, we predict that a migration of water between the poles is possible during periods of low obliquity (<35°) and that the pole favoring accumulation is controlled by the timing of perihelion. Not more than several meters of ice could have exchanged this way between the caps. This pole-to-pole migration is thus unlikely to have participated in building the upper 350 m of the north polar cap. Additional results indicate significant changes in the dust lifting pattern when perihelion argument is reversed. In particular, a more uniform dust opacity cycle is predicted, with a drastic reduction of lifting around perihelion. When averaged over precession cycle, this reduced potential for dust lifting subsequently forces a clearer northern summer season, forcing the latter to remain colder than southern summer, and thus to exhibit lower condensation levels of water in the tropics where water is carried to the south. With a colder northern summer on a precession-cycle average, advection of water to the southern hemisphere is less efficient than the opposite transfer during southern summer. Such asymmetry in the cross-equatorial transport of water combines with the northward orientation of circulation forced by topography to reduce deposition of volatiles in the south relative to the deposition of volatiles in the opposite hemisphere, thereby providing a powerful differentiation mechanism consistent with the disparity of landforms between the poles.

[47] While the results presented here are robust with respect to the dust cycle, they only represent part of the climatic response associated with precession changes. In particular, it will be important to determine how the dust and water cycles are coupled to each other, including cloud microphysics and radiative effects, and what effect such coupling has on the net meridional exchange of water between hemispheres. It would also be useful to include the regolith as an exchangeable reservoir of water to elucidate its possible role in the large difference in resurfacing ages of the PLD. Finally, a critical step will be accomplished once the formation mode and the effects of dust lags will be properly represented in climate models. Such process holds the key to our understanding of the layering process in the polar regions.

[48] **Acknowledgments.** The authors wish to thank Michael Mischna and an anonymous reviewer for their constructive criticism of the manuscript. Part of the paper was written while F.M. was holding a National Research Council award to conduct research at the NASA Ames Research Center.

References

Bibring, J.-P., et al. (2004), Perennial water ice identified in the south polar cap of Mars, *Nature*, *428*, 6983, 627–630.

Boynton, W. V., et al. (2002), et al Distribution of hydrogen in the near surface of Mars: Evidence for subsurface ice deposits, *Science*, *297*, 81–85.

Byrne, S., and A. P. Ingersoll (2003), A sublimation model for Martian south polar ice features, *Science*, *299*, 1051–1053.

Clancy, R. T., A. W. Grossman, M. J. Wolff, P. B. James, D. J. Rudy, Y. N. Billawala, B. J. Sandor, S. W. Lee, and D. O. Muhleman (1996), Water vapor saturation at low latitudes around aphelion: A key to Mars climate?, *Icarus*, *122*, 36–62.

Colaprete, A., J. R. Barnes, R. M. Haberle, M. Robert, J. L. Hollingsworth, H. H. Kieffer, and T. N. Titus (2005), Albedo of the south pole on Mars determined by topographic forcing of atmosphere dynamics, *Nature*, *435*, 184–188.

Forget, F., F. Hourdin, R. Fournier, C. Hourdin, O. Talagrand, M. Collins, R. L. Stephens, P. L. Read, and J.-P. Huot (1999), Improved general circulation models of the Martian atmosphere from the surface to above 80 km, *J. Geophys. Res.*, *104*, 24,155–24,176.

Forget, F., R. M. Haberle, F. Montmessin, B. Levrard, and J. W. Head (2006), Formation of glaciers on Mars by atmospheric precipitation at high obliquity, *Science*, *311*, 368–371.

Haberle, R. M., C. B. Leovy, and J. B. Pollack (1982), Some effects of global dust storms on the atmospheric circulation of Mars, *Icarus*, *50*, 322–367.

Haberle, R., M. Joshi, J. Murphy, J. Barnes, J. Schofield, G. Wilson, M. Lopez-Valverde, J. Hollingsworth, A. Bridger, and J. Schaeffer (1999), General circulation model simulations of the Mars Pathfinder atmospheric structure investigation/meteorology data, *J. Geophys. Res.*, *104*, 8957–8974.

Haberle, R. M., C. P. McKay, J. Schaeffer, M. Joshi, N. A. Cabrol, and E. A. Grin (2000), Meteorological control on the formation of Martian paleolakes, *Annu. Lunar Planet. Sci. Conf.*, *XXXI*, Abstract 1509.

Haberle, R. M., J. R. Murphy, and J. Schaeffer (2003), Orbital change experiments with a Mars general circulation model, *Icarus*, *161*, 66–89.

Haberle, R. M., M. A. Kahre, J. R. Murphy, P. R. Christensen, and R. Greeley (2006), Role of dust devils and orbital precession in closing the Martian dust cycle, *Geophys. Res. Lett.*, *33*, L19S04, doi:10.1029/2006GL026188.

Herkenhoff, K. E., and J. J. Plaut (2000), Surface ages and resurfacing rates of the polar layered deposits on Mars, *Icarus*, *144*, 243–253.

Houben, H., R. M. Haberle, R. E. Young, and A. P. Zent (1997), Modeling the Martian seasonal water cycle, *J. Geophys. Res.*, *102*, 9069–9084.

Jakosky, B. M., B. G. Henderson, and M. T. Mellon (1993), The Mars water cycle at other epochs: Recent history of the polar caps and layered terrain, *Icarus*, *102*, 286–297.

Kahre, M. A., J. R. Murphy, and R. M. Haberle (2006), Modeling the Martian dust cycle and surface dust reservoirs with the NASA/Ames general circulation model, *J. Geophys. Res.*, *111*, E06008, doi:10.1029/2005JE002588.

Kieffer, H. H. (1979), Mars south polar spring and summer temperatures: A residual CO_2 frost, *J. Geophys. Res.*, *84*, 8263–8288.

Kieffer, H. H., S. C. Chase, T. Z. Martin, R. E. Miner, and F. D. Palluconi (1976), Martian North Pole summer temperatures—Dirty water ice, *Science*, *194*, 1341–1344.

Laskar, J., B. Levrard, and J. F. Mustard (2002), Orbital forcing of the Martian polar layered deposits, *Nature*, *419*, 375–377.

Laskar, J., A. C. M. Correia, M. Gastineau, F. Joutel, B. Levrard, and P. Robutel (2004), Long term evolution and chaotic diffusion of the insolation quantities of Mars, *Icarus*, *170*, 343–364.

Levrard, B., F. Forget, F. Montmessin, and J. Laskar (2004), Recent ice-rich deposits formed at high latitudes on Mars by sublimation of unstable equatorial ice during low obliquity, *Nature*, *431*, 1072–1075.

Mellon, M. T., and B. M. Jakosky (1993), Geographic variations in the thermal and diffusive stability of ground ice on Mars, *J. Geophys. Res.*, *98*, 3345–3364.

Milkovich, S. M., and J. W. Head III (2005), North polar cap of Mars: Polar layered deposit characterization and identification of a fundamental climate signal, *J. Geophys. Res.*, *110*, E01005, doi:10.1029/2004JE002349.

Mischna, M. A., and M. I. Richardson (2005), A reanalysis of water abundances in the Martian atmosphere at high obliquity, *Geophys. Res. Lett.*, *32*, L03201, doi:10.1029/2004GL021865.

Mischna, M. A., M. I. Richardson, R. J. Wilson, and D. J. McCleese (2003), On the orbital forcing of Martian water and CO_2 cycles: A general circulation model study with simplified volatile schemes, *J. Geophys. Res.*, *108*(E6), 5062, doi:10.1029/2003JE002051.

Montmessin, F., F. Forget, P. Rannou, M. Cabane, and R. M. Haberle (2004a), Origin and role of water ice clouds in the Martian water cycle

as inferred from a general circulation model, *J. Geophys. Res.*, *109*, E10004, doi:10.1029/2004JE002284.

Montmessin, F., R. M. Haberle, and F. Forget (2004b), Transport of water ice to the Martian south pole 25,000 years ago, *Bull. Am. Astron. Soc.*, *36*, 1170.

Montmessin, F., T. Fouchet, and F. Forget (2005), Modeling the annual cycle of HDO in the Martian atmosphere, *J. Geophys. Res.*, *110*, E03006, doi:10.1029/2004JE002357.

Newman, C. E., S. R. Lewis, P. L. Read, and F. Forget (2002), Modeling the Martian dust cycle: 1. Representations of dust transport processes, *J. Geophys. Res.*, *107*(E12), 5123, doi:10.1029/2002JE001910.

Newman, C. E., S. R. Lewis, and P. L. Read (2005), The atmospheric circulation and dust activity in different orbital epochs on Mars, *Icarus*, *174*, 135–160.

Plaut, J. J., R. Kahn, E. A. Guinness, and R. E. Arvidson (1988), Accumulation of sedimentary debris in the south polar region of Mars and implications for climate history, *Icarus*, *76*, 357–377.

Richardson, M. I., and R. J. Wilson (2002a), Investigation of the nature and stability of the Martian seasonal water cycle with a general circulation model, *J. Geophys. Res.*, *107*(E5), 5031, doi:10.1029/2001JE001536.

Richardson, M. I., and R. J. Wilson (2002b), A topographically forced asymmetry in the Martian circulation and climate, *Nature*, *416*, 298–301.

Richardson, M. I., R. J. Wilson, and A. V. Rodin (2002), Water ice clouds in the Martian atmosphere: General circulation model experiments with a simple cloud scheme, *J. Geophys. Res.*, *107*(E9), 5064, doi:10.1029/2001JE001804.

Smith, M. D. (2002), The annual cycle of water vapor on Mars as observed by the Thermal Emission Spectrometer, *J. Geophys. Res.*, *107*(E11), 5115, doi:10.1029/2001JE001522.

Smith, M. D. (2004), Interannual variability in TES atmospheric observations of Mars during 1999–2003, *Icarus*, *167*, 148–165.

Thomas, P. C., M. C. Malin, P. B. James, B. A. Cantor, R. M. E. Williams, and P. Gierasch (2005), South polar residual cap of Mars: Features, stratigraphy, and changes, *Icarus*, *174*, 535–559.

Titus, T. N., H. H. Kieffer, and P. R. Christensen (2003), Exposed water ice discovered near the south pole of Mars, *Science*, *299*, 1048–1051.

J.-P. Bibring and Y. Langevin, Institut d'Astrophysique Spatiale, Universite Paris Sud-Orsay, Orsay Campus, Batiment 120, F-91405 Orsay Cedex, France.

R. T. Clancy, Space Science Institute, P.O. Box 3075, Bald Head Island, NC 28461, USA.

F. Forget, Laboratoire de Météorologie Dynamique, CNRS/IPSL/UPMC, Universite Paris 6, BP 99, F-75005 Paris Cedex 05, France.

R. M. Haberle, Space Science Division, NASA Ames Research Center, MS 245-3, Moffett Field, Mountain View, CA 94035-1000, USA.

F. Montmessin, Service d'Aéronomie du CNRS/IPSL/UVSQ, Réduit de Verrières, Route des Gatines, F-91371 Verrières le Buisson Cédex, France. (franck.montmessin@aero.jussieu.fr)